Bipedal walking: quasi-ballistic single-support phase, double-support under finite joint torques

Yannick Aoustin, Alexander Formalskii

Bipedal walking: quasi-ballistic single-support phase, double-support under finite joint torques

Yannick Aoustin[1*] and Alexander Formalskii[2†]

[1]LS2N UMR CNRS 6004, Nantes Université-École Centrale Nantes, CNRS, UMR 6004, 1 rue de la Noë, Nantes, F-44000, Pays de La Loire, France.

[2]Institute of Mechanics, Lomonosov Moscow State University, 1 Mitchurinskii Prospect, Nantes, Moscow, 119192, , Russia.

*Corresponding author(s). E-mail(s): Yannick.Aoustin@univ-nantes.fr;
Contributing authors: formal@imec.msu.ru;
†These authors contributed equally to this work.

Abstract

Among the numerous studies devoted to simulating human walking, very few take into account a non-instantaneous double support phase, i.e., one spread over a non-zero time interval. And yet this double support phase plays an important role, if only for the overall stability of the movement. A new periodic walking motion is proposed for a planar biped with quasi-ballistic single-support phases, where only the ankle of the supporting foot is actuated, and double-support phases with synchronized rotations of the feet, one around the heel and the other around the toes. The biped consists of a torso, two identical legs with knees, and massless feet. The synthesis of this walking period is based on a step that includes a single support phase and a double support phase.The quasi-ballistic movement is calculated by numerically solving a boundary value problem, taking two velocities into account. The initial velocities of the biped and the initial and final orientations of the foot of the pendulum leg are the unknowns in this boundary value problem. A velocity constraint is applied to the ankle of the foot just before it leaves the ground to prevent any unwanted contact rebound, and a velocity constraint is applied to the same ankle at the end of the movement to prevent the heel from impacting the ground. The double support phase begins as soon as the heel of the front foot touches the ground. The foot then rotates around its heel until it is flat on the ground. The rear foot begins to rotate around its toes in preparation for lifting off the ground. During this support phase, the ankle, knee, and hip joints are actuated by six motors. The six torques are

piecewise constant functions whose values are the unknowns in an optimization problem designed to ensure the periodicity of the walking. Numerical results from the walking synthesis illustrate the approach. It is possible to see a video with animation of the design of bipedal walking in this paper, using reference here. These numerical results are also compared with human walking data, freely available.

1 Introduction

There are very few studies devoted to bipedal walking that include a non-instantaneous double support phase extending over a non-zero time interval. However, this double support phase plays an important role, if only to ensure the overall stability of the movement. Furthermore, it is physically impossible to achieve periodic walking using only ballistic movements in single support. However, electromyography studies have shown that the leg muscles are relatively inactive during this swing phase [1]. The objective of this article is to combine a double support phase and a single support oscillation phase based on a quasi-ballistic movement in order to achieve periodic walking for a flat biped, inspired by human walking. Passive bipeds, which are moved by gravity over a shallow slope, can adopt a regular gait quite comparable to human walking. Among many studies, McGeer [2] was one of the forerunners in this field. He has investigated the physical conditions enabling a 2D biped with semicircular knees and feet but no trunk to perform periodic passive walking. Beletskii [3] studied different problems about the dynamics and control of bipedal walking of humans, birds, and dinosaurs. Borzova and Hurmuzlu [4] have analyzed the dynamics of a five-link biped with knees and upper body. They have detected three limit cycles that include three distinct upper body motions. There is also in their paper an investigation on the structural stability of these cycles and a demonstration that erected body posture is only achievable when torsional springs are placed in the hip joints. Numerous papers are devoted to the analysis of human walking and the identification of its characteristics, [5, 6]. Interesting studies can be found on the walking cycle, with a wealth of information such as the decomposition of a walking cycle, displacements of the center of mass CoM, of the center of pressure CoP, typical profiles of ground reaction components [5]. Winter [6] brings together a wealth of information on techniques for recording and studying the physical parameters of muscles, forces, and moments of the human body. To elucidate possible foot pathology the trajectory of the CoP is described and interpreted for several foot positions in [7]. For one leg, the sequence of swing and stance phases constitutes the complete human gait cycle. The swing phase begins when the toes of the swing leg touch down, and continues until the foot of this leg returns to the ground and touches it by the heel. Mochon and McMahon [8, 9] have rigorously demonstrated that during the swing phase, the movement of the transfer leg can be determined solely by the effects of gravity. More recently to design a power-capable knee prosthesis with ballistic swing-phase Culver *et al* [10] use the property that during walking of a healthy human the swing-phase knee motion has a passive behavior. The time of the double-support movement is close to 20% of the time of

the step [11, 12]. Therefore, for different problem statements, the design of a periodic walk with a cycle consisting of a ballistic swing phase and an instantaneous double-support with impulsive torques makes sense [13–15]. In these publications, impulsive torques, applied in the joints at the double-support phase are described by Dirac delta-functions. The problem of the walking control for a planar biped robot, with minimal energy expenditure is considered in [16]. It is shown that the movement with any prescribed average speed is either ballistic or on the straight legs, with impulse control at the start and end of the support phases. However, the double-support phase for human walking is distributed in time and its time cannot be neglected. Blajer and Schiehlen [17] addressed the synthesis of control for bipedal walking without impact, which consists of single-support phases and double-support phases. To avoid impacts a specific biped movement and a force control to manage ground reaction are synthesized. Rostami *et al*. [18] used the principle of optimal control to define a walking trajectory without impact, with single-support phases and double-support phases. This method, complex to implement, is very rigorous in finding the optimal solution with constraints. However, the torques required are of the bang-bang type and put a lot of strain on the actuators. Miossec and Aoustin [19] have shown, using a Poincaré map, that for a controlled biped with pointed feet, the double-support phase improves the orbital stability of a walking without impact. Joint trajectories are defined as functions of the orientation angle of the supporting shin instead of time. Tan *et al* [20] also proposed a finite time double-support starting with a foot contact and the other foot resting on the toe, the aim being for the trunk to remain upright. More recently, Hobon *et al* [21] define the range of achievable speeds for two walking movements for a particular planar biped robot, which differ in the definition of their finite-time double-support phases. For each speed, these two walking movements are numerically obtained using a parametric optimization algorithm, as a function of a sthenic criterion. This list of papers is far from exhaustive. However, to our best knowledge, there are currently no contributions concerning walking with a ballistic swing phase and a double-support phase with finite torques in the joints. This paper aims to fill this gap.

Unlike the articles [13, 15, 22] and monograph [14], a walking without impact is considered here. The cycle of this walk without impact is composed of a single-support phase with a quasi-ballistic motion and a double-support phase distributed in *finite time*. This cycle is designed for a 2D biped model with a trunk, and two identical legs, each with one knee, and one foot without mass. The hypothesis of a foot without mass is common; see [23]. This hypothesis is natural because it is based on the fact that the mass of a human foot is approximately equal to 0.7 kg, [24]. This mass is small compared to the total mass of the human leg. In the single-support phase, the biped's movement is ballistic, except in the ankle joint of the supporting leg, where torque is applied to keep the (massless) foot of the supporting leg in balance. A boundary value problem is solved to define this quasi-ballistic motion with position and velocity conditions to achieve the desired final biped configuration and avoid impulsive impacts.

The double-support movement begins when the heel of the front foot touches the ground and the other (rear) foot rests on the toe. During the movement of double-support, both feet rotate in the same direction, the front foot around its heel and

the rear foot around its toe. The biped's locomotor system thus forms a closed structure with the ground. The definition of the double-support phase can be seen as the following boundary value problem: The initial joint variables, their velocities from the previous single-support phase, and the final joint variables, their velocities at the end of double-support movement, are known from the definition of the single-support phase. To solve this boundary value problem, the components Γ_i with $i = 1, 2, 3, 4, 5, 6$ of the torque vector $\mathbf{\Gamma}$ are defined as piecewise constant functions over time T_{DS} of the double-support motion. Unilateral constraints are satisfied throughout the walking movement. The double-support phase ends with the rear foot, which was on the toe, lifting off, and the front foot lying flat. The designed double-support movement represents nearly 20% of the step time. The ankle flexion values of the leg in the stance position, just before its foot is lifted off the ground for the swing and when its foot touches the ground with the heel, are close to the ankle's range of motion during human walking, see [25]. Furthermore, in double-support the rear foot and the front foot rotate in the same sense, respectively, around its toe and heel. Based on these observations, the double-support movement can therefore be considered similar to that involved in human walking.

The paper is summarized as follows. Section 2 presents the original walking movement of the biped. The mathematical model of the biped is described in section 3. Section 4 is dedicated to the statement of the boundary value problem to define quasi-ballistic movement in single-support. The statement of the inverse dynamic problem to define the double-support movement is described in section 5. The numerical results are shown and discussed in section 6. Section 7 offers our conclusion and perspectives.

2 The walking movement

The biped periodic walking consists of phases of single-support and double-support distributed over time. During quasi-ballistic movement in single-support phase, the torques in all interlink joints are zero, with the exception of the torque in the ankle joint of the supporting leg. Torque is applied to the ankle joint of the supporting leg to keep the foot in balance. During the movement of single-support, since the feet are massless, the torque applied to the ankle of the swinging leg is equal to zero. The orientation of the sole of the swinging foot can therefore be arbitrarily chosen to be parallel to the ground. During the movement of double-support, the torques are applied to the six joints; during this time, both feet rotate: the foot of the rear leg − around its toe, the foot of the front leg − around its heel. To explain our statement of the problem more clearly, Fig. 1 shows several stick-figures, which result from our numerical investigations.

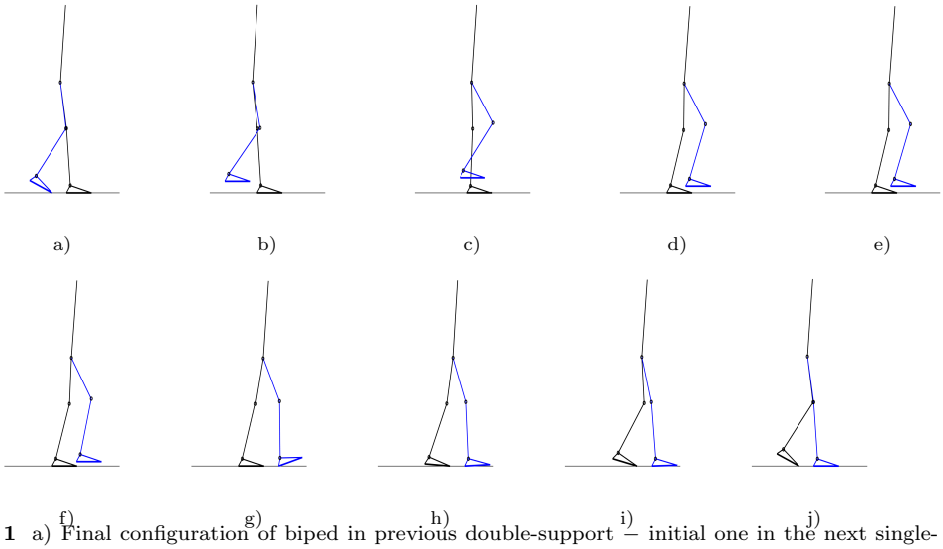

Fig. 1 a) Final configuration of biped in previous double-support − initial one in the next single-support; b) - f) Intermediate configurations in single-support; g) Final configuration in single-support − initial one in the next double-support; h) - i) Intermediate configurations in double-support; j) Final configuration in double-support − initial one in the next single-support movement.

In Fig. 1 one can see that the stick-figure j) coincides with the stick-figure a), but the legs are swapped. During the single-support movement the foot of the supporting leg is flat (see the stick-figures a) - g)). The distance between the toe of the rear leg and the heel of the front leg at the times, when both legs are in contact with the ground, is the same, see the stick-figures g) - j). The times T_{SS} of the single-support movement and T_{DS} of the double-support movement also remain unchanged from step to step. As a result, this walking is considered as a periodic process.

3 Mathematical model of the biped walking

The absolute orientations of the shins and thighs are defined with the angle variables q_1, q_2, q_3, and q_4 (see Fig. 2). They describe the deviations of the shins and thighs from the vertical line. These angles are positive if the deviations are directed counter-clockwise. The orientation of the trunk is defined by angle q_5. Cartesian coordinates of the hip joint are x and y. Thus, the vector $\mathbf{x}$ of the generalized coordinates of a biped with massless feet is $\mathbf{x} = [q_1, q_2, q_3, q_4, q_5, x, y]^\top$. The superscript $^\top$ means transposition. The orientations of the two massless feet are described by the angles q_{p1} and q_{p2} (see Fig. 2).

The mathematical model of the biped is:

$$\mathbf{A}(\mathbf{x})\ddot{\mathbf{x}} + \mathbf{H}(\mathbf{x}, \dot{\mathbf{x}})\dot{\mathbf{x}} + g\mathbf{G}(\mathbf{x}) = \mathbf{D}\boldsymbol{\Gamma} + \mathbf{J}_{\mathbf{r}_1}^\top \mathbf{r}_1 + \mathbf{J}_{\mathbf{r}_2}^\top \mathbf{r}_2, \tag{1}$$

where $\mathbf{A}(\mathbf{x})$ is a 7×7 symmetric positive definite inertia matrix, $\mathbf{H}(\mathbf{x}, \dot{\mathbf{x}})$ is a 7×7 matrix, which defines the centrifugal and Coriolis forces, $g\mathbf{G}(\mathbf{x})$ is a 7×1 vector to

represent the torques due to the gravity force, g is the gravity acceleration. $\mathbf{D}$ is a 7×6 matrix, which is composed of 0 and ±1. $\mathbf{\Gamma}$ is the 6×1 vector of the six joint torques applied by the biped. These six torques are applied in the hip-, knee-, and ankle-joints. $\mathbf{J}_{\mathbf{r}_1}$ and $\mathbf{J}_{\mathbf{r}_2}$ are Jacobian matrices, which are defined from the contact condition with the ground (2). Vectors $\mathbf{r}_i = (r_{ix}, r_{iy})^\top$, with $i = 1,\ 2$, are ground reactions applied to massless feet and therefore to the ankle-joints. The matrices of the mathematical model (1) are introduced in the Appendix of the paper.

Let $V_{\mathbf{a}_i}$ be the linear velocity of the ankle joint of leg i ($i = 1,\ 2$, see Fig. 2) as follows:

$$V_{\mathbf{a}_i} = \mathbf{J}_{\mathbf{r}_i}\dot{\mathbf{x}}, \tag{2}$$

$$\dot{V}_{\mathbf{a}_i} = \mathbf{J}_{\mathbf{r}_i}\ddot{\mathbf{x}} + \dot{\mathbf{J}}_{\mathbf{r}_i}\dot{\mathbf{x}}. \tag{3}$$

It is assumed that there is no sliding or take-off movement of the supporting legs. To avoid sliding movement, the friction between the feet and the support surface must be sufficiently large. To avoid the take-off of the supporting legs, the vertical components of the ground reactions must be directed upwards.

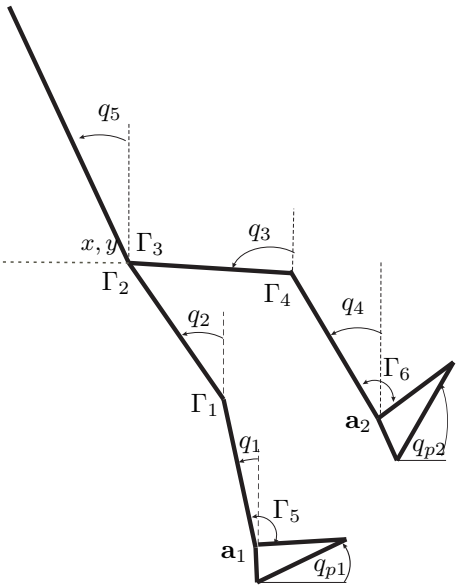

Fig. 2 Generalized coordinates, and interlink torques.

In the previous references [13–15], bipedal walking is considered with an instantaneous double support phase. The bipedal configurations at the beginning and end of the double support phase are therefore identical, except for a simple inversion of the legs between the two configurations. For real human walking, the double-support movement is distributed over time, and consequently, the configuration of the human at the end of the double-support movement differs from the configuration at the start of this movement. Consequently, for the walking in 2D considered here in order to

approximate human walking, the configurations at the start and end of the single-support movement are also different. But the step length (for a healthy human) is always the same as in our model (see Figs. 1 and 3).

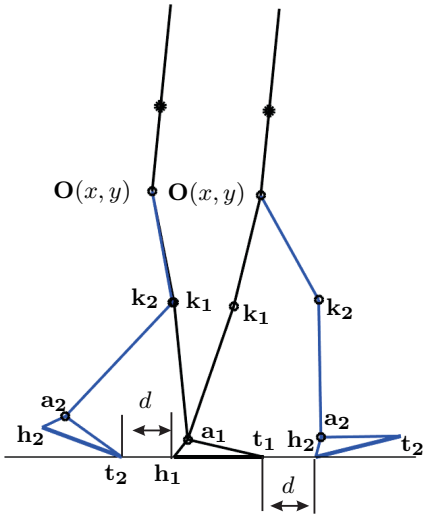

Fig. 3 Initial and final configurations of the single-support movement.

In the following for numerical investigations, the anthropomorphic parameters are used for a person of mass M = 75 kg and height 1.82 m. Table 1 shows the numerical values used for the parameters of the bipedal links: their masses, lengths, moments of inertia, and the positions of their centers of mass. The geometric definition of the positions of the centers of mass of a biped with its feet is specified in Figs. 4 and 6. Moments of inertia are defined in relation to the hip joint for the trunk and thighs and in relation to the knee joints for the shins.

Table 1 Physical parameters of the biped.

	Mass (kg)	Length (m)	Inertia moment (kg·m^2)	Position of Centers of mass (m)
Human shin	$m_s = 4.6$	$l_s = 0.45$	$I_s = 0.12$	$s_s = 0.162$
Human thigh	$m_t = 8.6$	$l_t = 0.55$	$I_t = 0.22$	$s_t = 0.384$
Human trunk	$m_T = 48.6$	$l_p = 0.75$	$I_T = 4.0$	$s_T = 0.386$
Foot, CoP excursion	$m_f = 0.0$	$l_f = 0.04$ $L_f = 0.22$ $l_y = 0.07$	$I_f = 0.00$	

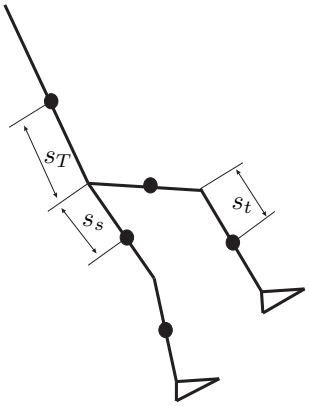

Fig. 4 Position of the centers of mass of the trunk, shin, and thigh.

4 Single-support movement: boundary value problem

Here we describe the general statement of the boundary value problem for designing a quasi-ballistic single-support movement of a biped with massless feet.

4.1 Definition of the desired movement in single support of the biped with massless feet

Recall that at [13–15, 22] the single-support ballistic motion of the five-link biped without feet is considered. The initial angular velocities in the five joints are found to transfer this biped during a given time from a given initial configuration to a given terminal configuration. The boundary value problem is solved numerically using the algorithm of Rosenbrock. However, here we have to take into account the presence of

the massless feet. In this case, the statement of the problem becomes different. First, a torque is applied to the ankle of the supporting leg to move its CoP from the heel to the toe of the stance foot. As a result, there is no tilting of the support foot on the ground during the single-support phase. We assume that due to friction between the sole of the supporting leg and the ground, the supporting stance foot cannot slide along the support, also that the weight of the biped is compensated by the vertical component of the ground reaction, and there is no motion of the supporting foot in the vertical direction. Second, to ensure that the rear foot rises from the ground without impact, the linear velocity $V_{\mathbf{a_2}}$ of the ankle $\mathbf{a_2}$ is prescribed to be orthogonal to the segment $\mathbf{a_2t_2}$, see Fig. 5. Third, to obtain a soft landing (without collision) of the ankle $\mathbf{a_2}$ its linear velocity $V_{\mathbf{a_2}}$ at the end of single-support must be orthogonal to the segment $\mathbf{a_2h_2}$, see Fig. 5.

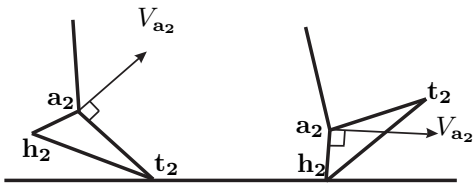

Fig. 5 The velocity vector $V_{\mathbf{a_2}}$ of the ankle joint $\mathbf{a_2}$ must be orthogonal to segment $\mathbf{a_2t_2}$ at the rising of massless foot and must be orthogonal to segment $\mathbf{a_2h_2}$ at the landing of this foot.

4.2 Design of the quasi-ballistic movement

The design of the quasi-ballistic movement of a biped with massless feet is described in more detail in this section. In the single-support phase, the movement is performed on the supporting leg, Figs. 1 (see stick-figures a), b), c), e)) and 3. Assume that leg 1 is the supporting leg and that, during the single-support movement, $q_{p1}(t) \equiv 0$. Thus, the foot of leg 1 is a motionless foot with a flat foot contact. It is assumed that during single-support movement, the interlink torques $\Gamma_i = 0$, $i = 1, \cdots, 4,\ 6$ (see Fig. 2). But the torque $\Gamma_5 \neq 0$. Therefore, we call the single-support motion a quasi-ballistic one. This torque is applied to the ankle joint $\mathbf{a_1}$ between the shin and the foot of the supporting leg. This torque is applied to both the foot and the shin. If torque Γ_5 is applied to the shin in a counterclockwise direction, that is, in the positive direction, then the same torque, in absolute value, is applied to the foot in a clockwise direction, that is, in the opposite direction (negative) and *vice versa*. This torque acts on the ankle joint $\mathbf{a_1}$ to compensate for the influence of the ground reaction $\mathbf{r}_1$. In other words, the torque Γ_5 is calculated to ensure that the foot is in flat contact with the ground and, therefore, is balanced. According to Fig. 6a, the equilibrium condition of the flat massless foot, i.e., its static balance) of the support leg 1 is:

$$\Gamma_5 = l_x(t) r_{1y} + l_y r_{1x}. \tag{4}$$

With function $l_x(t)$ we describe (prescribe) in expression (4) the movement of the CoP along the sole from the heel ($l_x(0) = -l_f$) to the toe ($l_x(T_{SS}) = L_f$), l_y is the

constant height of the ankle joint above the support, Fig. 6a. Now let us introduce the dimensionless time $\tau = t/T_{SS}$ and define the function $l_x(t)$

$$l_x(t) = -l_f + \psi(\tau)\,(L_f + l_f)\,, \tag{5}$$

with $\psi(\tau)$ as a fourth-order polynomial function that defines the following intermediate condition $\psi(1/2) = 1/2$ with initial and final positions $\psi(0) = 0$, $\psi(1) = 1$, and with initial and final velocities $\dot{\psi}(0) = 0$, $\dot{\psi}(1) = 0$. Fig. 6b shows the function $l_x(t)$ with numerical values of l_f and L_f, which are summarized in Table 1. The variable l_x increases over time in a strictly monotonic way.

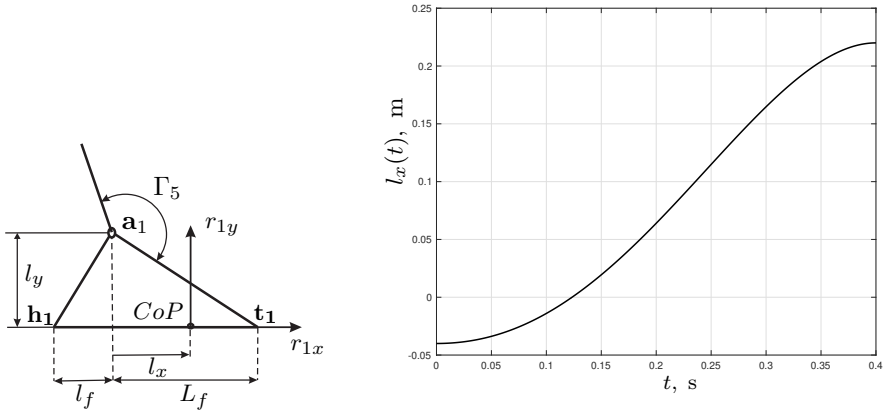

a) b)

Fig. 6 a) Size characteristics of the foot: l_f is the distance between the heel $\mathbf{h}_1$ and the vertical projection of the ankle joint $\mathbf{a}_1$ on the sole, L_f is the distance between this projection and the toe $\mathbf{t}_1$, function $l_x = l_x(t)$ describes the movement of the CoP along the sole. Moment Γ_5 is applied in the ankle joint $\mathbf{a}_1$ between the shin and foot. b) function $l_x(t)$.

4.3 Dynamic model taking into account the ground reaction during the quasi-ballistic movement

In the single-support movement on the leg 1, the linear velocity $V_{\mathbf{a_1}}$ of the ankle joint $\mathbf{a}_1$ identically equals to zero, therefore (see equations (2) and (3)):

$$V_{\mathbf{a_1}} = \mathbf{J}_{\mathbf{r}_1}\dot{\mathbf{x}} \equiv 0 \tag{6}$$

and

$$\dot{V}_{\mathbf{a_1}} = \mathbf{J}_{\mathbf{r}_1}\ddot{\mathbf{x}} + \dot{\mathbf{J}}_{\mathbf{r}_1}\dot{\mathbf{x}} \equiv 0 \tag{7}$$

Ten scalar equations are represented by the expressions (1), (4), and (7) to find ten unknown variables that are the seven components of the acceleration vector $\ddot{\mathbf{x}}$, the two components of the ground reaction $\mathbf{r}_1$ applied to the supporting shin, and the torque Γ_5 applied to the shin, appearing due to the ground reaction $\mathbf{r}_1$.

The following system of the differential equations groups differential equations (1), equation (4), and differential equations (7):

$$\begin{bmatrix} \mathbf{A}(\mathbf{x}) & -\mathbf{d}_5 l_y + \mathbf{j}_{\mathbf{r}_{11}}^\top & -\mathbf{d}_5 l_x + \mathbf{j}_{\mathbf{r}_{12}}^\top \\ \mathbf{J}_{\mathbf{r}_1} & \mathbf{0}_{2\times 1} & \mathbf{0}_{2\times 1} \end{bmatrix} \begin{bmatrix} \ddot{\mathbf{x}} \\ r_{1x} \\ r_{1y} \end{bmatrix} = \begin{bmatrix} -\mathbf{H}(\mathbf{x}, \dot{\mathbf{x}})\dot{\mathbf{x}} - g\mathbf{G}(\mathbf{x}) \\ -\dot{\mathbf{J}}_{\mathbf{r}_1}\dot{\mathbf{x}} \end{bmatrix}. \quad (8)$$

Here $\mathbf{d}_5$ is the fifth column of the matrix $\mathbf{D}$; $\mathbf{j}_{\mathbf{r}_{11}}$ and $\mathbf{j}_{\mathbf{r}_{12}}$ are the first and second lines of the Jacobian matrix $\mathbf{J}_{\mathbf{r}_1}$ (see Appendix). The system (8) contains nine scalar equations.

For the ankle joint $\mathbf{a_2}$ of the transfer leg, we define the following boundary conditions:

- The first condition ensures that the ankle $\mathbf{a_2}$ of the rear foot rises from the ground without any impact:
$$V_{\mathbf{a_2}}(0) \cdot \mathbf{t_2 a_2}(0) = 0. \quad (9)$$
Equation (9) means that velocity vector $V_{\mathbf{a_2}}(0)$ is orthogonal to vector $\mathbf{t_2 a_2}(0)$. In this case, the velocity vector $V_{\mathbf{a_2}}(0)$ can be written as follows:
$$V_{\mathbf{a_2}}(0) = \begin{bmatrix} y_{\mathbf{t_2}}(0) - y_{\mathbf{a_2}}(0) \\ x_{\mathbf{a_2}}(0) - x_{\mathbf{t_2}}(0) \end{bmatrix} \dot{q}_{p2}(0).$$
Here $\dot{q}_{p2}(0)$ is the angular velocity of the rear foot rotation around the toe $\mathbf{t_2}$ at the start ($t = 0$) of the single-support movement – simultaneously with the end of the previous double-support movement. Equation (9) can be rewritten under the following extended form:
$$\dot{x}_{\mathbf{a_2}}(0)(x_{\mathbf{a_2}}(0) - x_{\mathbf{t_2}}(0)) + \dot{y}_{\mathbf{a_2}}(0)(y_{\mathbf{a_2}}(0) - y_{\mathbf{t_2}}(0)) = 0. \quad (10)$$

- The second boundary condition ensures a soft (without collision) landing of the ankle $\mathbf{a_2}$ at the end of the single-support movement:
$$V_{\mathbf{a_2}}(T_{SS}) \cdot \mathbf{h_2 a_2}(T_{SS}) = 0. \quad (11)$$
Equation (11) means that velocity vector $V_{\mathbf{a_2}}(T_{SS})$ is orthogonal to vector $\mathbf{h_2 a_2}(T_{SS})$. In this case, the velocity vector $V_{\mathbf{a_2}}(T_{SS})$ can be written as follows:
$$V_{\mathbf{a_2}}(T_{SS}) = \begin{bmatrix} y_{\mathbf{h_2}}(T_{SS}) - y_{\mathbf{a_2}}(T_{SS}) \\ x_{\mathbf{a_2}}(T_{SS}) - x_{\mathbf{h_2}}(T_{SS}) \end{bmatrix} \dot{q}_{p2}(T_{SS}).$$
Here $\dot{q}_{p2}(T_{SS})$ is the angular velocity of the front foot rotation around the heel $\mathbf{h_2}$ at the end ($t = T_{SS}$) of the single-support movement – simultaneously at the beginning of the next double-support movement. Equation (11) can be rewritten under the following extended form:
$$\dot{x}_{\mathbf{a_2}}(T_{SS})(x_{\mathbf{a_2}}(T_{SS}) - x_{\mathbf{h_2}}(T_{SS})) + \dot{y}_{\mathbf{a_2}}(T_{SS})(y_{\mathbf{a_2}}(T_{SS}) - y_{\mathbf{h_2}}(T_{SS})) = 0. \quad (12)$$

4.4 The unknown variables to be determined in order to solve the boundary value problem and thus the quasi-ballistic movement

Let d denote the distance between the toe $\mathbf{t_2}$ of the rear leg 2 and the heel $\mathbf{h_1}$ of the front leg 1 at the initial moment $t = 0$ of the single-support movement (see Fig. 3). The distance between the toe $\mathbf{t_1}$ of supporting leg 1 and the heel $\mathbf{h_2}$ of transfer leg 2 at the last moment $t = T_{SS}$ of the single-support movement must be the same (for a healthy human). At the initial instant $t = 0$ knowing the distance d, the angles $q_{p1}(0) = 0$, $q_1(0)$, $q_2(0)$, it is possible to find the coordinates $x(0)$, $y(0)$ of the hip joint $\mathbf{O}$ (see Fig. 3) with a direct geometric model of the part of two links $(\mathbf{a_1k_1O})$ of supporting leg 1. Knowing the coordinates $x(0)$, $y(0)$, and the angle $q_{p2}(0)$, the angles $q_3(0)$, $q_4(0)$ can be found using the inverse geometric model of the two-link part $(\mathbf{a_2k_2O})$ of transfer leg 2, Fig. 3. The initial configuration of the biped can then be completely determined if the angle $q_5(0)$ of the trunk orientation is also given. Similarly, at the given final instant $t = T_{SS}$ of the movement on a single-support, knowing the same distance d and the angles $q_{p1}(T_{SS}) = 0$, $q_1(T_{SS})$, $q_2(T_{SS})$, we can find the coordinates $x(T_{SS})$, $y(T_{SS})$ of the hip joint $\mathbf{O}$ with a direct geometric model of the two-link part $(\mathbf{a_1k_1O})$ of the supporting leg 1, Fig. 3. Afterward, knowing the coordinates $x(T_{SS})$, $y(T_{SS})$, and the angle $q_{p2}(T_{SS})$, the angles $q_3(T_{SS})$, $q_4(T_{SS})$ can be determined using the inverse geometric model of the two-link part $(\mathbf{a_2k_2O})$ of the transfer leg 2. The final configuration of the biped can then be fully determined if the angle $q_5(T_{SS})$ is also defined.

The distance d and the step time T_{SS} are parameters to solve the boundary value problem. This means that their values are given and do not change while solving the boundary value problem (this problem is solved numerically by using an iteration process). Another important point is that the initial and final configurations of the transfer leg are recalculated after each iteration, but the boundary configurations of the supporting leg and the orientations of the trunk are fixed. The matter is that the angles $q_{p2}(0)$ and $q_{p2}(T_{SS})$ are unknown values and change during the iteration process. Thus, in addition to the changes in values $q_{p2}(0)$ and $q_{p2}(T_{SS})$, the boundary configurations of the transfer leg must be recalculated. Therefore, the boundary value problem to be solved is specific. We have the set of initial configurations of the transfer leg, parameterized by a single parameter – by angle $q_{p2}(0)$. There is also the set of final configurations of the transfer leg, parameterized by a single parameter – by angle $q_{p2}(T_{SS})$. The five initial velocities $\dot{q}_i(0)$ $(i = 1, \cdots, 5)$, the initial $q_{p2}(0)$ and final $q_{p2}(T_{SS})$ angles of the orientations of the massless foot 2 satisfying two conditions (10) and (12), imposed on the velocities of the ankle joints, are calculated to reach the final configuration of the biped starting from the initial one (see Fig. 3). In this way, the boundary value problem can be solved. We emphasize that we find not only the initial angular velocities of the links but also the initial and final configurations of the transfer leg of the biped. In other words, we find simultaneously five initial angular velocities and two orientation angles of the feet to "connect" the initial and final configurations of the biped.

To summarize the boundary value problem, starting from the initial configuration $q_i(t=0) = q_i^{initial}$, $i = 1, \cdots, 5$ let us find the seven unknown variables

$$\mathcal{P} = (\dot{q}_1(0),\ \dot{q}_2(0),\ \dot{q}_3(0),\ \dot{q}_4(0),\ \dot{q}_5(0),\ q_{p2}(0),\ q_{p2}(T_{SS}))^\top \tag{13}$$

in order to satisfy the two conditions (10) and (12) about the orientation of the linear velocity V_{a_2}, respectively at the initial time ($t = 0$) and final time ($t = T_{SS}$) of the single-support phase and the five conditions $q_i(t = T_{SS}) = q_i^{final}$, $i = 1, \cdots, 5$.

The function *fsolve* of Matlab ® with *trust-region-dogleg* algorithm, which is inspired by the Newton-Raphson method, is used here to solve the boundary value problem described above numerically. At each iteration, this algorithm *fsolve* converges by modifying the numerical value of each component of (13) to the solution of the boundary value problem, and $q_3(t = 0)$, $q_4(t = 0)$, $q_3(t = T_{SS})$, and $q_4(t = T_{SS})$ are recalculated as a function of the numerical values of $q_{p2}(0)$ and $q_{p2}(T_{SS})$.

Remark: To calculate the initial conditions for the motion equations (8) the toe $\mathbf{t_1}$ is chosen as the origin of the coordinates.

5 Double-support movement: Problem definition

At the end of the single-support phase, the change of orientation of the transferred foot is operated instantaneously due to our model with massless feet. The landing foot without mass touches the ground with its heel, Fig. 1 g).

The other foot keeps in contact with the ground through its toe. The front leg is leg 2, but the rear leg is leg 1. In the double-support phase, both feet rotate, Figs. 1 d), 7. The double-support movement stops when the front foot is flat on the ground and the rear foot is lifted off the ground, Fig. 1 e). At this instant, the single-support movement of the next step begins.

The torque vector Γ has now six components

$$\Gamma = \left[\, \Gamma_1\ \Gamma_2\ \Gamma_3\ \Gamma_4\ \Gamma_5\ \Gamma_6 \,\right]^\top \tag{14}$$

to actuate the following joint angles:

$$\begin{array}{l} \theta_1 = q_2 - q_1,\ \ \theta_2 = q_5 - q_2,\ \ \ \theta_3 = q_5 - q_3, \\ \theta_4 = q_3 - q_4,\ \theta_5 = q_{p1} - q_1,\ \theta_6 = q_{p2} - q_4. \end{array} \tag{15}$$

The torques Γ_5, Γ_6 depend on the ground reactions $\mathbf{r}_1$ and $\mathbf{r}_2$. They can be represented by the following conditions of the equilibrium of the massless feet (see similar condition (4)):

$$\begin{array}{c} \Gamma_5 = (x_{\mathbf{t_1}} - x_{\mathbf{a_1}})r_{1y} - (y_{\mathbf{t_1}} - y_{\mathbf{a_1}})r_{1x}, \\ \Gamma_6 = (x_{\mathbf{h_2}} - x_{\mathbf{a_2}})r_{2y} - (y_{\mathbf{h_2}} - y_{\mathbf{a_2}})r_{2x}. \end{array} \tag{16}$$

In the double-support movement taking into account equations (2), (3) and contacts with the ground of the toe $\mathbf{t_1}$ and heel $\mathbf{h_2}$ (see Fig. 7) the equations of unilateral constraints in velocity and acceleration are, respectively:

- in velocity:

$$V_{\mathbf{a_1}} = \mathbf{J}_{\mathbf{r}_1}\dot{\mathbf{x}} \equiv \begin{bmatrix} L_f \mathrm{sin} q_{p1} - l_y \mathrm{cos} q_{p1} \\ -L_f \mathrm{cos} q_{p1} - l_y \mathrm{sin} q_{p1} \end{bmatrix} \dot{q}_{p1}, \equiv \mathbf{J}_{\mathbf{q_{p1}}}\ \dot{q}_{p1}, \tag{17}$$

$$V_{\mathbf{a_2}} = \mathbf{J}_{\mathbf{r}_2}\dot{\mathbf{x}} \equiv \begin{bmatrix} -l_f \mathrm{sin} q_{p2} - l_y \mathrm{cos} q_{p2} \\ l_f \mathrm{cos} q_{p2} - l_y \mathrm{sin} q_{p2} \end{bmatrix} \dot{q}_{p2}, \equiv \mathbf{J}_{\mathbf{q_{p2}}}\ \dot{q}_{p2}. \tag{18}$$

- in acceleration:

$$\dot{V}_{\mathbf{a_1}} = \mathbf{J}_{\mathbf{r}_1}\ddot{\mathbf{x}} + \dot{\mathbf{J}}_{\mathbf{r}_1}\dot{\mathbf{x}} \equiv \mathbf{J}_{\mathbf{q_{p1}}}\ \ddot{q}_{p1} + \dot{\mathbf{J}}_{\mathbf{q_{p1}}}\ \dot{q}_{p1}, \tag{19}$$

$$\dot{V}_{\mathbf{a_2}} = \mathbf{J}_{\mathbf{r}_2}\ddot{\mathbf{x}} + \dot{\mathbf{J}}_{\mathbf{r}_2}\dot{\mathbf{x}} \equiv \mathbf{J}_{\mathbf{q_{p2}}}\ \ddot{q}_{p2} + \dot{\mathbf{J}}_{\mathbf{q_{p2}}}\ \dot{q}_{p2}. \tag{20}$$

.

The design of the double support phase is also a boundary value problem that can be defined as follows: Starting from the initial configuration and initial velocity of the biped, which are the configuration and velocity of the biped at the end of the previous single-support phase, how do we define the motion of the biped to reach the final configuration and final velocity of the biped, which are the configuration and velocity of the biped at the start of the next single-support phase? The solution to this boundary value problem must satisfy the following unilateral constraints at the toe $\mathbf{t_1}$ and heel $\mathbf{h_2}$:

$$r_{1y} > 0 \text{ and } r_{2y} > 0. \tag{21}$$

The proposed approach here is to search for trajectories generated by piecewise constant torques during the double-support phase. Roussel *et al* [26] proposed a similar strategy for a complete periodic walking of a biped but with a simplified dynamic model. The inertia matrix was assumed to be constant and diagonal, and centripetal accelerations were ignored. The same authors have shown that this strategy provides movements with lower input energy compared to polynomial or Fourier extensions [27]. The non-zero components $\Gamma_i(t)$ with $i = 1, 2, 3, 4, 5, 6$ of the torque vector $\mathbf{\Gamma}$ are defined with piecewise constant functions Γ_{ik} $(k = 1, \cdots, N)$ during time T_{DS} of the double-support phase such as each component $\Gamma_i(t)$ is:

$$\Gamma_i(t) = \Gamma_{ik} \quad \text{for} \quad T_{SS} + (k-1)\frac{T_{DS}}{N} \leq t < T_{SS} + k\frac{T_{DS}}{N},\ k = 1, \cdots, N \tag{22}$$

Taking into account of the equations (1), (16), (19), and (20) a parametric optimization problem under the unilateral constraints (21).

From numerical results, which are presented in the next section 6, we observed that no additional constraints are necessary to lead the optimization algorithm.

The piecewise constant values of the six torques Γ_i are the optimization variables, and the criterion is expressed as follows:

$$\begin{aligned} J_{crit} = \sum_{i=1}^{6}(\theta_i(T_{SS}+T_{DS}) - \theta_i^{des}(T_{SS}+T_{DS}))^2 + \\ + \sum_{i=1}^{6}(\dot{\theta}_i(T_{SS}+T_{DS}) - \dot{\theta}_i^{des}(T_{SS}+T_{DS}))^2 \end{aligned} \tag{23}$$

Here exponent *des* means *desired*. These equations (1), (16), (19), and (20) are grouped to form a system (1) that is expressed in the Appendix. With the knowledge of its right part the system (1) is solved at each time to find $\ddot{\mathbf{x}}$, $\ddot{q}_{p1}$, $\ddot{q}_{p2}$, $\mathbf{r}_1$, and $\mathbf{r}_2$. The vectors $\dot{\mathbf{x}}$, $\mathbf{x}$, and variables $\dot{q}_{p1}$, $\dot{q}_{p2}$, q_{p1}, and q_{p2} are calculated by numerical integration with the Runge-Kutta algorithm.

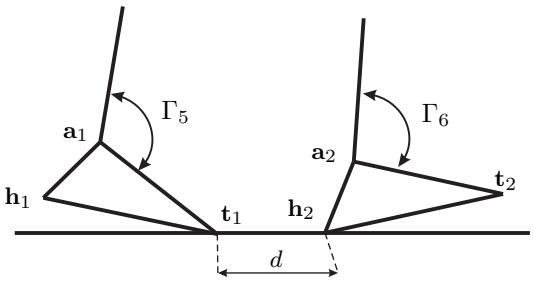

Fig. 7 Double-support movement, rear foot (leg 1) and front foot (leg 2)

The function *fmincon* of Matlab® with the *Sequential Quadratic Programming* algorithm, which consists in determining parameters that minimize a function, here (23), while respecting equality or/and inequality constraints, here (21), on these parameters, is used to solve the boundary value problem for the double-support motion.

6 Numerical results

In Subsection 6.1 the results of the movement of the single-support, which is a solution of the boundary value problem, are described. The subsection 6.2 contains the results of the investigation of the double-support movement.

6.1 Single-support movement

To solve the boundary value problem, the following values $d = 0.15$ m and $T_{SS} = 0.4$ s are given. In the walk obtained, the values of the initial and final trunk orientations are equal to $-4°$. The trunk is therefore slightly inclined forward. The initial and final orientations of the massless foot 2 are respectively $q_{p2}(0) \approx -27.26°$ and $q_{p2}(T_{SS}) \approx$

18.81°. These numerical values are consistent with the biomechanics observation of walking. Indeed, if we consider the corresponding values of the ankle flexions $q_{p2}(0) - q_4(0) \approx 6.93°$ and $q_{p2}(T_{SS}) - q_4(T_{SS}) \approx 18.14°$ there are close to the ankle range of motion during a human walking, see Perry and Burnfield [25], page 53. The orientations $q_{p2}(0)$ and $q_{p2}(T_{SS})$ are two components of the solution vector of the boundary value problem. The numerical values of the five other components of the solution vector are the following angular velocities:

$$\dot{q}_1(0) = -0.08923 \text{ rd/s}, \quad \dot{q}_2(0) = -1.84635 \text{ rd/s}, \quad \dot{q}_3(0) = 2.20698 \text{ rd/s},$$

$$\dot{q}_4(0) = -2.10673 \text{ rd/s}, \quad \dot{q}_5(0) = 0.34110 \text{ rd/s}.$$

With the knowledge of $q_{p2}(0)$, $q_{p2}(T_{SS})$, d, and the chosen numerical values of $q_1(0)$, $q_2(0)$ $q_1(T_{SS})$, and $q_2(T_{SS})$, such as:

$$q_1(0) = 4.1°,\ q_2(0) = 8.1°,\ q_1(T_{SS}) = 14.0°,\ q_2(T_{SS}) = -10.0°,$$

the initial and final configurations are determined by solving an inverse geometric model to find $q_3(0)$, $q_4(0)$, $q_3(T_{SS})$, and $q_4(T_{SS})$, which are equal:

$$q_3(0) = 7.4°,\ q_4(0) = -34.2°,\ q_3(T_{SS}) = 21.8°,\ q_4(T_{SS}) = 0.7°.$$

The results concerning the quasi-ballistic single-support motion of the biped are presented by the stick-figures a), b), c) in Figure 1. The graphs of the ground reaction, torque Γ_5 in the ankle joint of the supporting leg are presented together with the results of the double-support movement in Subsection 6.2. The designed quasi-ballistic motion looks human-like because the transfer leg (swing) moves above the ground, the legs bend with knees forward, the trunk does not fall down (despite the lack of moment in the hip joint) and oscillates slightly near the vertical line once per step. These "human" features have not been prescribed beforehand in the statement of the problem. Perhaps, they are intrinsic features of the quasi-ballistic motion.

6.2 Double-support movement

The numerical value of time T_{DS} of the double-support movement is equal to 0.1 s. This means that the percentage of the finite time T_{DS} of the double-support movement, with respect to the time $T_{SS} + T_{DS}$ of one walking step, is equal to 20%, which is close to the characteristics of human walking (see [11, 12]). The results concerning the double-support movement of the biped are presented by the stick figures c), d), and e) in Fig. 1. Unilateral constraints are always satisfied as can be seen from the curves of the two vertical components of the ground reactions $\mathbf{r}_i$ (i = 1, 2), see Fig. 8. In this figure, the vertical line at the time instant $t = 0.4$ s means the end of the single-support and the beginning of the double-support.

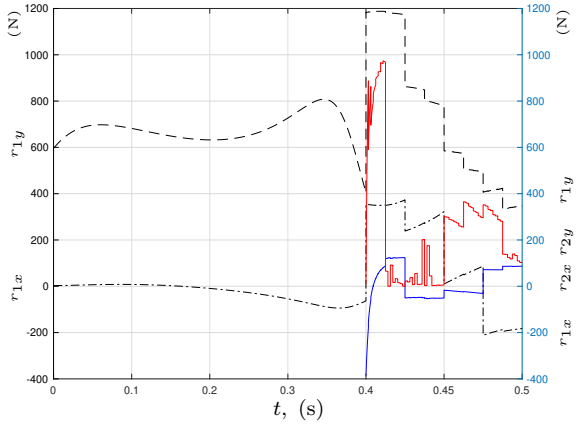

Fig. 8 Components following $x-$ axis and $y-$ axis of the ground reactions acting in the two feet during a half step: Components r_{1x} in dashdot line and r_{1y} in dashed line for the supporting leg in single-support ($0\text{ s} < t < 0.4\text{ s}$) and for the same leg in double-support ($0.4\text{ s} < t < 0.5\text{ s}$). Components r_{2x} in solid blue line, and r_{2y} in solid red line for the transfer leg that becomes the second support leg at $t = 0.4$ s, r_{2x} and r_{2y}. *Remark: the time scale of the double-support phase is twice that of the single-support phase.*

As shown in Fig. 8, the vertical components r_{1y} and r_{2y} of the ground reactions r_1 and r_2 are always positive. This means that the legs do not lose contact with the ground during either single-support or double-support movements.

Figure 9 shows the knee variables $\theta_1 = q_2 - q_1$ and $\theta_4 = q_3 - q_4$ as functions of time t during the double stance movement of $0.4\text{ s} < t < 0.5$ s. Both functions are always positive. This means that a reverse knee bend of both legs is avoided during the double-support phase.

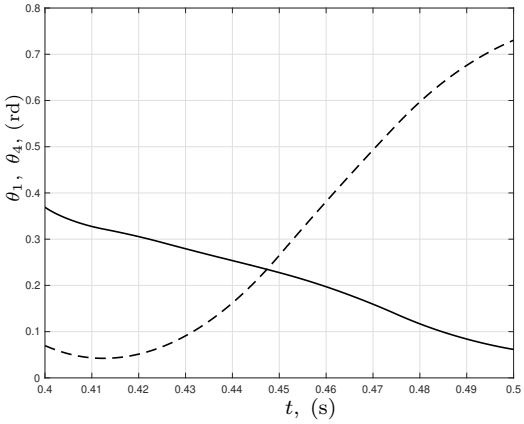

Fig. 9 The knee joint variables $\theta_1 = q_2 - q_1$ (dashed line), $\theta_4 = q_3 - q_4$ (solid line) of the legs during the double-support phase.

In Fig. 10 the absolute evolution of the trunk inclination is plotted for one step. The trunk is always oriented forward. The condition of periodicity is well satisfied, its initial orientation is equal to its final one. The magnitude of the trunk movement remains very small. During one step it makes two oscillations near the vertical line and angle q_5 changes in the interval $-4.47° < q_5 < -3.44°$.

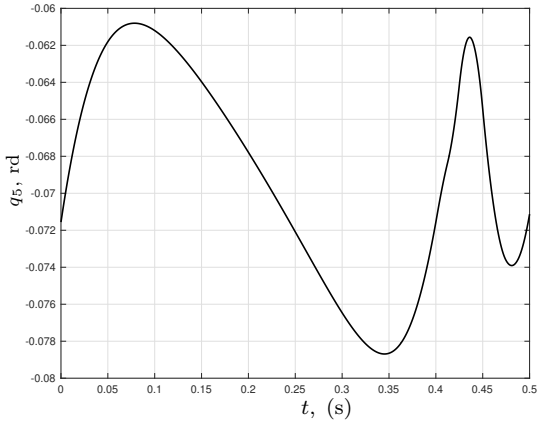

Fig. 10 Profile of the absolute evolution (in radians) of the trunk orientation during a step.

Fig. 11 shows the torque Γ_5 in the ankle joint of leg 1 during single-support and double-support movements. The CoP travels along the sole of the supporting foot during the single-support movement and stays on the toe of this foot during the double-support phase. The ground reaction is applied to this toe during the double-support

phase. At the beginning of the double support phase, the change in the structure of the model leads to a discontinuity in each of the torques. We observe that the torque applied to the ankle of the rear leg increases sharply until it reaches a value close to 750 N. This observation is consistent with the numerical values of the normal components r_{1y} of the reaction force acting on the toe of the rear foot. This seems physically coherent because the biped pushes on the rear leg to move forward during the double-support phase.

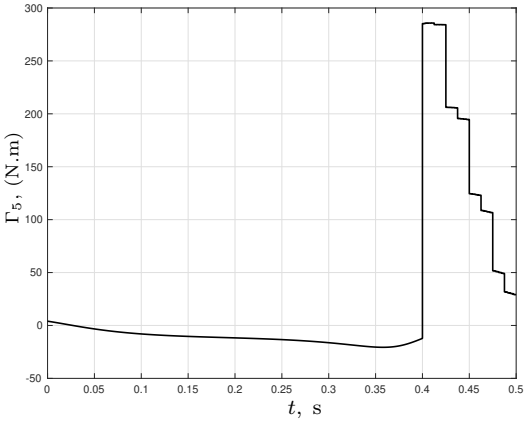

Fig. 11 Profile of the ankle torque Γ_5 of the rear leg.

Figure 12a) shows the evolution of the angles q_{p1} and q_{p2} during the double-support phase. The function q_{p1} is negative throughout the time interval (0.4 s $< t <$ 0.5 s) and decreases in this time interval strictly monotonically. The function q_{p2} is positive in this time interval, initially decreasing strictly monotonically and then oscillating around a small positive value with low amplitude. In Fig. 12b) the torque Γ_5 applied to the ankle joint of the rear leg is much greater than the torque Γ_6 applied to the ankle joint of the front leg. In Fig. 8, we can see a significant value, close to 1000 N for the r_2y component of the ground reaction force applied to the heel of the front foot. However, the amplitude of Γ_6 torque is smaller than the amplitude Γ_5. This is understandable given that, for a foot, the ankle is closer to the heel than to the toe. This confirms that the biped pushes on the rear leg to move forward during the double-support phase.

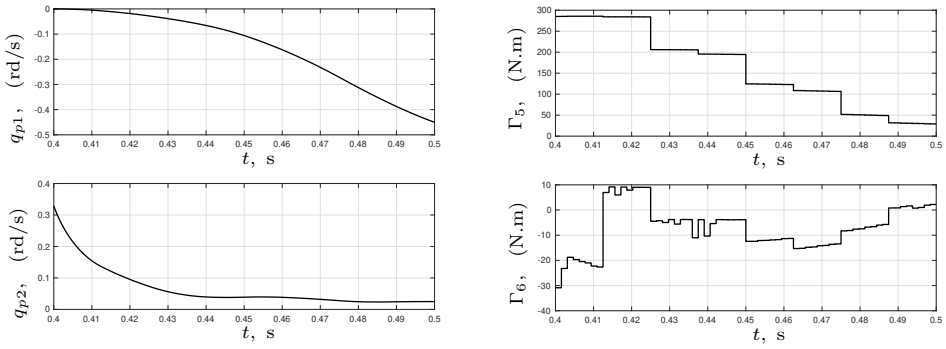

a) b)

Fig. 12 Front leg and rear leg in double-support phase: a) Orientation angles of feet (in radians). b) Ankle torques.

On Figure 13, the two angular velocities $\dot{q}_{p1}$ and $\dot{q}_{p2}$ are shown at the time interval (0.4 s $< t <$ 0.5 s). The function $\dot{q}_{p1}$ is negative during this interval. The velocity $\dot{q}_{p2}$ is also initially negative, but increases and at a certain instant t becomes zero, after oscillating around zero with a small amplitude. This means that the orientations of both feet follow a monotonic behavior, i.e., the rear foot and the front foot rotate in the same sense, respectively, around its toe and heel. This monotonic behavior of q_{p1} and q_{p2} is confirmed by Figure 12a). It is consistent with human walking; see [25].

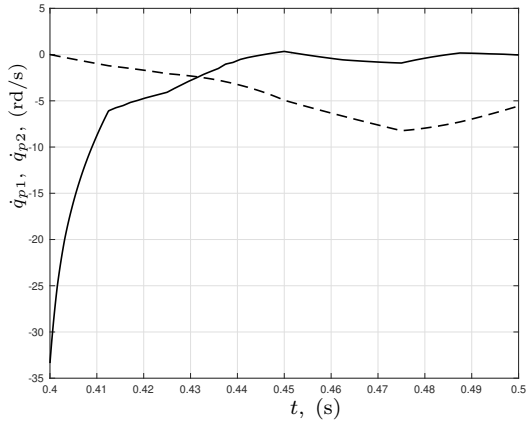

Fig. 13 The velocities $\dot{q}_{p1}$ (dashed line) and $\dot{q}_{p2}$ (solid line) of the two-foot soles to the ground during the double-support phase.

In Fig. 14 the interlink torques Γ_1, Γ_2, Γ_3, and Γ_4 are presented as functions of time during the double-support movement. These torques are discontinuous functions.

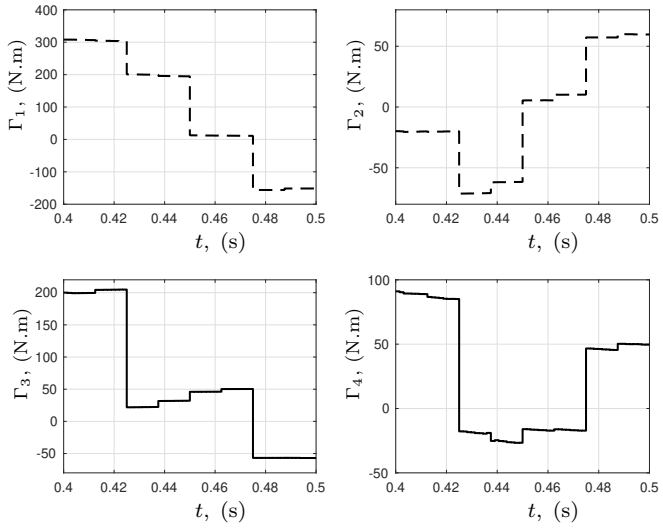

Fig. 14 Four joint torques during the double-support movement: in front leg (solid lines), in rear leg (dashed lines).

We stopped our calculation when the numerical value of the criterion (23) was approximately $7.1 \cdot 10^{-4}$. This criterion is obtained with 64 optimization variables for each torque, i.e., $64 \times 6 = 384$ optimization variables for the set of the six torques. When we look at the torque profiles, Figs. 12b and 14, only the profile of Γ_6 shows the different 64 values of the optimized variables. However, they do exist for the other couples, but the numerical differences between them mean that they are hardly visible graphically. The optimization algorithm has favored the torque on the ankle of the front leg as the most determinant. A video of the complete walking trajectory is obtained from the simulation of our mathematical model with the parameters, which are gathered in Table 1. This video is available here.

The torques applied to the joints of both legs during the quasi-ballistic movement in single-support phase are zero, with the exception of the torque applied to the ankle joint of the supporting leg, which is non-zero and varies continuously over time.

During movement in double-support the control torques are applied to the joints of both legs in the form of a piecewise constant as a function of time. Under such control torques, the angular accelerations at the joints also undergo discontinuities. However, the angular velocities remain continuous in time along with the angles.

As it follows from the above, bipedal walking under the designed control algorithm is smooth, and this smoothness may be seen, for example, in animation.

6.3 Comparison of some characteristics of synthesized walking with that of a healthy human

The animation made it possible to visualize the bio-inspired property of the synthesized walking of the bipedal robot equipped with massless feet. To confirm this observation, we compared the simulated data of biped walking with those of a healthy human being using data obtained from the following open science platform [28]. These data were derived from a protocol of experiments involving different walking speeds performed by ten healthy subjects are presented [29]. Subject number six was considered. His weight, 72.6 kg, is close to that of a biped (75 kg). The walking speed used as a reference is the minimum speed investigated 0.7 m/s. The walking condition was the preferred walking. The data are compared for one walking cycle, using the representation conventions of the experimental database. This is defined as the time between two heel strikes of the same leg on the ground. The considered data are the angular variables of the locomotor system, the intersegmental moments, normalized with respect to the body mass and the reaction forces in the sagittal plane. Figure 15, shows the evolution of the angular variables of the ankle, knee, and hip joints. The orders of magnitude of the values of these joint variables of the biped are close to those of the subject. At the beginning and end of the swing phase, we observe a discontinuity in the joint variable of the biped's ankle. This is due to the instantaneous movement of the massless foot, whose sole is fixed horizontally relative to the ground. Figure 16, halfway through the cycle, when the front foot strikes the ground, the normalized intersegmental moments of the ankle and knee of the biped's supporting leg reach values that are more than double those of the subject. The double support phases therefore drive bipedal walking in order to maintain a cyclic walking motion, with the swing phase being ballistic. We should also highlight the important role played by the muscles of the human lower limbs, some of which are biarticular, agonist, and antagonist, acting as actuators or shock absorbers. This difference is also likely due to the flexibility of the human arch, which allows for heel elevation and thus a variation in the contact surface of the supporting foot during the swing phase. This phenomenon has been excellently described by Rose and Gamble [5]. It was partially taken into account by Tlalolini *et al* [30] to define for a seven-body planar biped a cyclic motion that is composed of single-support phases that include a subphase of rotation of the supporting foot about the toe. Figure 17, the values of the anterior/posterior and vertical components are comparable in magnitude between the biped and the subject, except during double support. The vertical components correspond respectively to the weight of the biped and the subject. The sequence of phases in a cycle between the walking of the biped and the walking of the subject is practically the same.

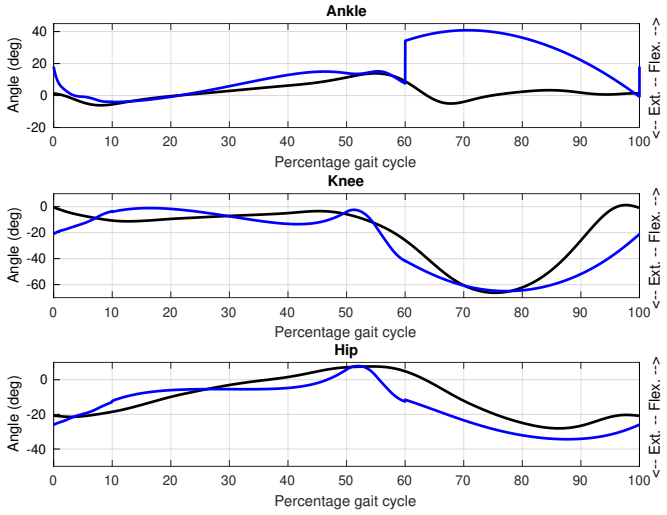

Fig. 15 Comparison of joint variables in the locomotor system (blue color) of biped with those of the subject (black color).

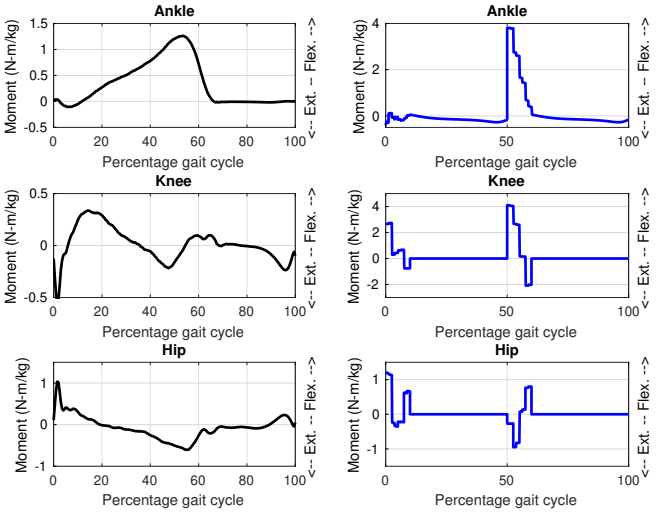

Fig. 16 Comparison of normalized intersegmental moment (blue color) of the biped system with those of the subject (black color).

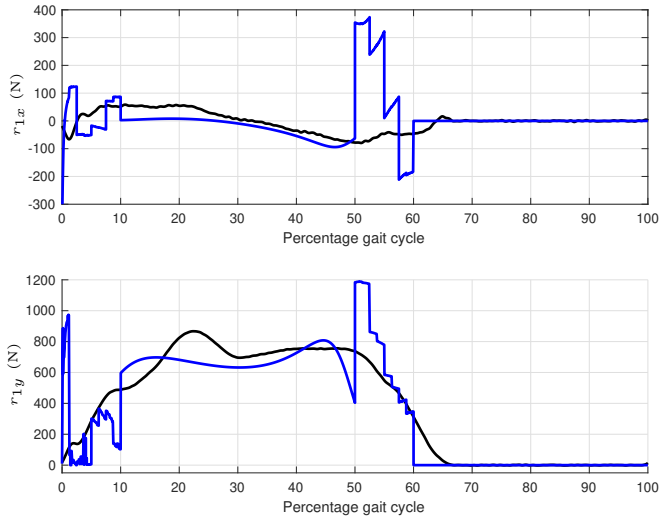

Fig. 17 Comparison of the ground reaction force (blue color) acting on the biped's supporting foot with those (black color) acting on the subject's supporting foot during a walking cycle.

De Coke *et al.* [31] have experimentally demonstrated that when a human being walks barefoot, the path of the *CoP* from the heel to the toes can be divided into four sub-phases: initial contact phase, forefoot contact phase, foot flat phase and forefoot push off phase. These results guided the choice of a non-linear progression of the trajectory (5) that was made in our study. Figure 18 shows the trajectory of the *CoP* in the sagittal plane for the biped and for Subject number six. There are notable differences between the two graphs. These differences are due to the fact that the duration of single support for our model and that of single support for the subject do not coincide. Furthermore, when walking, the foot in single support does not remain flat on the ground and its trajectory. And the trajectory of the *CoP* in humans also shifts slightly in the transverse plane of the supporting foot. However, the amplitudes of the two trajectories are of the same order of magnitude. The trajectory of the *CoP* calculated from the experimental data is also not linear either. Therefore, in the present study, the hypothesis that the trajectory of the *CoP* evolves according to a fourth-order polynomial function makes sense.

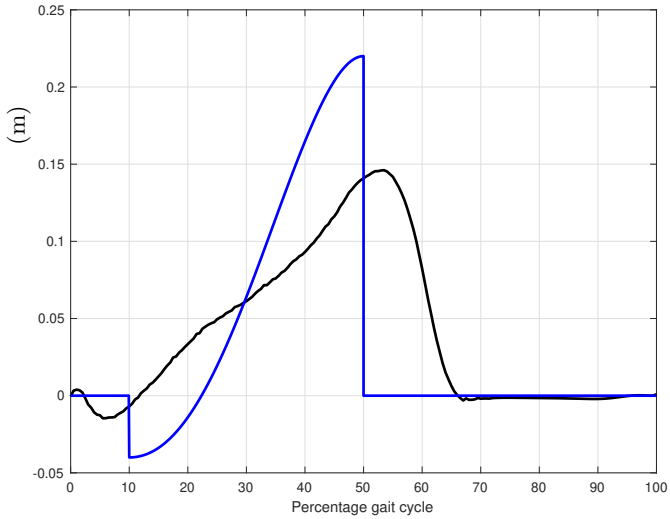

Fig. 18 Comparison of the trajectory of the *CoP* along the sole of the biped (blue color) and of the sole of the subject's foot during a walking cycle.

7 Conclusion

The definition of walking with a distributed in-time double-support is a complex problem [9, 19, 25]. In these references [13, 15, 22], a ballistic motion in single support, which is coupled with a double-support phase *instantaneous*, is studied. Torques in the biped's joints during the instantaneous double-support are impulsive. They are described by Dirac delta-functions.

Thanks to a planar biped with feet this paper theoretically shows that the periodic walking of a healthy human on a horizontal smooth ground can be organized with an original quasi-ballistic motion design of the single-support phase and a double-support motion with piecewise control torques applied in the leg joints.

The quasi-ballistic motion is designed by solving a boundary value problem with the aim of satisfying the boundary conditions of configuration and velocity. The velocity boundary conditions are related to the linear velocity of the ankle, ensuring that the transfer leg does not collide with the ground at the start and end of the single-support movement. A torque is applied at the ankle of the leg in stance, preventing the foot in stance from tipping on the ground, i.e., it keeps this foot balanced, supported, and flat on the ground. The torques at the other five interlink joints are identically equal to zero. This means that the single-support phase is not completely ballistic.

The double-support motion is distributed in time due to piecewise control torques. This finite-time double-support phase is designed by solving an optimization problem based on the dynamic model that explicitly takes into account the contact of the feet on the ground. The optimization variables are the torques, sampled with piecewise

constants. Unfortunately, we were unable to prove the existence of solutions to the boundary value problem for single-support and double-support movements. However, we have devised numerical solutions for both cases.

The original quasi-ballistic motion and the characteristic of *distribution in time* for double-support movements allow for a periodic walking with torques of finite magnitude.

In our statement of the problem, the length and time of the step are given. Due to that, it is possible to find a set of walking movements by varying the length and time of the step.

A comparison between the bipedal walking and the walking of a healthy subject over one cycle showed that the evolution of the joints variables were similar. In both cases, the vertical components of the ground reaction force are consistent in single support phase with respect to the biped and the subject, respectively. The torques and ground reaction forces during the double support phase are more important for the bipedal walking that for the subject. In the case of bipedal walking, the double support phase is the driving force that enables forward movement.

An objective for future research is to extend the study on an exoskeleton: how to evaluate the efforts developed by humans carrying a payload, see [32], [22].

8 Declarations

Financial interests: The authors have no relevant financial or non-financial interests to disclose.

Matrices of the mathematical model

Matrices $\mathbf{D}$ *and* $\mathbf{\Gamma}$*:*

$$\mathbf{D} = \begin{pmatrix} -1 & 0 & 0 & 0 & 1 & 0 \\ 1 & -1 & 0 & 0 & 0 & 0 \\ 0 & 0 & -1 & 1 & 0 & 0 \\ 0 & 0 & 0 & -1 & 0 & 1 \\ 0 & 1 & 1 & 0 & 0 & 0 \\ 0 & 0 & 0 & 0 & 0 & 0 \\ 0 & 0 & 0 & 0 & 0 & 0 \end{pmatrix}, \quad \mathbf{\Gamma} = \begin{pmatrix} \Gamma_1 \\ \Gamma_2 \\ \Gamma_3 \\ \Gamma_4 \\ \Gamma_5 \\ \Gamma_6 \end{pmatrix}$$

Jacobian matrix $\mathbf{J}_{\mathbf{r}_1}$*:*

$$\mathbf{J}_{\mathbf{r}_1} = \begin{pmatrix} l_s \cos q_1 & l_t \cos q_2 & 0 & 0 & 0 & 1 & 0 \\ l_s \sin q_1 & l_t \sin q_2 & 0 & 0 & 0 & 0 & 1 \end{pmatrix}$$

Jacobian matrix $\mathbf{J}_{\mathbf{r}_2}$*:*

$$\mathbf{J}_{\mathbf{r}_2} = \begin{pmatrix} 0 & 0 & l_t \cos q_3 & l_s \cos q_4 & 0 & 1 & 0 \\ 0 & 0 & l_t \sin q_3 & l_s \sin q_4 & 0 & 0 & 1 \end{pmatrix}$$

Vector $\mathbf{G}(\mathbf{x})$*:*

$$\mathbf{G}(\mathbf{x}) = \begin{pmatrix} m_s s_s \sin q_1 \\ (m_t s_t + m_s l_t) \sin q_2 \\ (m_t s_t + m_s l_t) \sin q_3 \\ m_s s_s \sin q_4 \\ -m_T s_T \sin q_5 \\ 0 \\ (2m_s + 2m_t + m_T) \end{pmatrix}$$

Symmetric positive definite inertia matrix $\mathbf{A}$*:*

$$\mathbf{A} = \begin{pmatrix} I_s + m_s s_s^2 & l_t m_s s_s \cos(q_1 - q_2) & 0 & 0 & 0 & m_s s_s \cos q_1 & m_s s_s \sin q_1 \\ l_t m_s s_s \cos(q_1 - q_2) & I_t + m_s l_t^2 + m_t s_t^2 & 0 & 0 & 0 & (m_t s_t + m_s l_t)\cos q_2 & (m_t s_t + m_s l_t)\sin q_2 \\ 0 & 0 & I_t + m_s l_t^2 + m_t s_t^2 & m_s s_s l_t \cos(q_3 - q_4) & 0 & (m_t s_t + m_s l_t)\cos q_3 & (m_t s_t + m_s l_t)\sin q_3 \\ 0 & 0 & m_s s_s l_t \cos(q_3 - q_4) & I_s + m_s s_s^2 & 0 & m_s s_s \cos q_4 & m_s s_s \sin q_4 \\ 0 & 0 & 0 & 0 & I_T + m_T s_T^2 & -m_T s_T \cos q_5 & -m_T s_T \sin q_5 \\ m_s s_s \cos q_1 & (m_t s_t + m_s l_t)\cos q_2 & (m_t s_t + m_s l_t)\cos q_3 & m_s s_s \cos q_4 & -m_T s_T \cos q_5 & 2m_s + 2m_t + m_T & 0 \\ m_s s_s \sin q_1 & (m_t s_t + m_s l_t)\sin q_2 & (m_t s_t + m_s l_t)\sin q_3 & m_s s_s \sin q_4 & -m_T s_T \sin q_5 & 0 & 2m_s + 2m_t + m_T \end{pmatrix}$$

Matrix $\mathbf{H}$ *defining the Coriolis and centrifugal forces:*

$$\mathbf{H} = \begin{pmatrix} 0 & m_s s_s l_t \dot{q}_2 \sin(q_1 - q_2) & 0 & 0 & 0 & 0\ 0 \\ -m_s s_s l_t \dot{q}_1 \sin(q_1 - q_2) & 0 & 0 & 0 & 0 & 0\ 0 \\ 0 & 0 & 0 & m_s s_s l_t \dot{q}_4 \sin(q_3 - q_4) & 0 & 0\ 0 \\ 0 & 0 & -m_s s_s l_t \dot{q}_3 \sin(q_3 - q_4) & 0 & 0 & 0\ 0 \\ 0 & 0 & 0 & 0 & 0 & 0\ 0 \\ -m_s s_s \dot{q}_1 \sin q_1 & -(m_t s_t + m_s l_t)\dot{q}_2 \sin q_2 & -(m_t s_t + m_s l_t)\dot{q}_3 \sin q_3 & -m_s s_s \dot{q}_4 \sin q_4 & m_T s_T \dot{q}_5 \sin q_5 & 0\ 0 \\ m_s s_s \dot{q}_1 \cos q_1 & (m_t s_t + m_s l_t)\dot{q}_2 \cos q_2 & (m_t s_t + m_s l_t)\dot{q}_3 \cos q_3 & m_s s_s \dot{q}_4 \cos q_4 & -m_T s_T \dot{q}_5 \cos q_5 & 0\ 0 \end{pmatrix}$$

System to define the movements of the double-support phase:

$$\begin{bmatrix} \mathbf{A}(\mathbf{x}) & \mathbf{0}_{7\times1} & \mathbf{0}_{7\times1} & -\mathbf{j}_{\mathbf{r}_1}^{\top} & -\mathbf{j}_{\mathbf{r}_2}^{\top} \\ \mathbf{J}_{\mathbf{r}_1} & -\mathbf{J}_{q1} & \mathbf{0}_{2\times1} & \mathbf{0}_{2\times2} & \mathbf{0}_{2\times2} \\ \mathbf{J}_{\mathbf{r}_2} & \mathbf{0}_{2\times1} & -\mathbf{J}_{q2} & \mathbf{0}_{2\times2} & \mathbf{0}_{2\times2} \\ \mathbf{0}_{1\times7} & \mathbf{0}_{1\times1} & \mathbf{0}_{1\times1} & \left[\, y_{a_1},\, l_f + L_f - x_{a_1} \,\right] & \mathbf{0}_{1\times2} \\ \mathbf{0}_{1\times7} & \mathbf{0}_{1\times1} & \mathbf{0}_{1\times1} & \mathbf{0}_{1\times2} & \left[\, y_{a_2},\, d + l_f + L_f - x_{a_2} \,\right] \end{bmatrix} \begin{bmatrix} \ddot{\mathbf{x}} \\ \ddot{q}_{p1} \\ \ddot{q}_{p2} \\ \mathbf{r}_1 \\ \mathbf{r}_2 \end{bmatrix} = \begin{bmatrix} \mathbf{D} \begin{pmatrix} \Gamma_1 \\ \Gamma_2 \\ \Gamma_3 \\ \Gamma_4 \\ \Gamma_5 \\ \Gamma_6 \end{pmatrix} - \mathbf{H}(\mathbf{x}, \dot{\mathbf{x}})\dot{\mathbf{x}} - g\mathbf{G}(\mathbf{x}) \\ -\dot{\mathbf{J}}_{\mathbf{r}_1}\dot{\mathbf{x}} + \dot{\mathbf{J}}_{\mathbf{q_{p1}}}\dot{q}_{p1} \\ -\dot{\mathbf{J}}_{\mathbf{r}_2}\dot{\mathbf{x}} + \dot{\mathbf{J}}_{\mathbf{q_{p2}}}\dot{q}_{p2} \\ \Gamma_5 \\ \Gamma_6 \end{bmatrix}. \quad (1)$$

References

[1] Mena, D., Mansour, J.M., Simon, S.R.: Analysis and synthesis of human swing leg motion during gait and its clinical applications. Journal of Biomechanics **14**, 823–832 (1981)

[2] McGeer, T.: Passive dynamic walking. Int. J. of Robotics Research **9**(2), 62–82 (1990)

[3] Beletskii, V.V.: Biped Walking. (In Russian), Monograph, Nauka, Moscow, Russia, 286 pages, 1984

[4] Borzova, E., Hurmuzlu, Y.: Passively walking five-link robot. Automatica **40**(4), 621–629 (2004) https://doi.org/10.1016/j.automatica.2003.10.015

[5] Rose, J., Gamble, G.: Human Walking, Third Edition. Lippincott Williams & Wilkins, 2006

[6] Winter, W.: Biomechanics and Motor Control of Human Movement. Fourth Edition, John Wiley & Sons, Inc., 2009

[7] Lugade, V., Kaufman, K.: Center of pressure trajectory during gait: A comparaison of four foot positions. Gait Posture **40**(1), 252–254 (2014)

[8] Mochon, S., McMahon, T.A.: Ballistic walking. Journal of Biomech **13**(1), 49–57 (1980)

[9] Mochon, S., McMahon, T.A.: Ballistic walking: An improved model. Mathematical Bio-sciences **52**, 241–260 (1981)

[10] Culver, C., Vailati, L., Goldfarb, M.: A power-capable knee prosthesis with ballistic swing-phase. IEEE Transactions on Medical Robotics and Bionics **4**(4), 1034–1045 (2022) https://doi.org/10.1109/TMRB.2022.3216475

[11] Bogdanov, V.A.: Elements of Biomechanics of Human Body, pp. 5–37. In: Physiology of Motions (In Russian), Nauka: Leningrad, (1976)

[12] Bogdanov, V.A., Gurfinkel, V.S.: Biomechanics of Human Locomotion, pp. 276–315. In: Physiology of Motions (In Russian), Nauka: Leningrad, (1976)

[13] Formal'skii, A.M.: Motion of anthropomorphic biped under impulsive control. In: Proc. of Institute of Mechanics, Moscow State Lomonosov University: "Some Questions of Robot's Mechanics and Biomechnics", pp. 17–34 (1978, (In Russian))

[14] Formalskii, A.M.: Locomotion of Anthropomorphic Mechanisms. [In Russian], Monograph, Nauka, Moscow, Russia, 368 pages, 1982

[15] Formal'skii, A.M.: Ballistic walking design via impulsive control. ASCE, Journal of Aerospace Engineering **23**(2), 129–138 (2010)

[16] Bolotin, V.V.: Energetically optimal gaits of a biped robot. Izvestia of the USSR Academy of Sciences, Solid State Mechanics (In Russian) (6), 48–55 (1984)

[17] Blajer, W., Schiehlen, W.: Walking without impacts as a motion/force control problem. Transaction of the ASME **114**(4), 660–665 (1992) https://doi.org/10.1115/1.2897738

[18] Rostami, M., Bessonnet, G., Sardin, P.: Optimal gait synthesis of a planar biped. In: Proc. of the IFAC Motion Control, Grenoble, France, pp. 165–170 (1998)

[19] Miossec, S., Aoustin, Y.: A simplified stability study for a biped walk with underactuated and overactuated phases. International Journal of Robotics Research **24**(6), 537–551 (2005)

[20] Tan, M., Jenning, L., Wang, S.: Analysing human walking using dynamic optimisation, pp. 1–34 (2015)

[21] Hobon, M., De.León.Gómez, V., Abba, G., Aoustin, Y., Chevallereau, C.: Feasible speeds for two optimal periodic walking gaits of a planar biped robot. Robotica **40**(2), 377–402 (2022) https://doi.org/10.1017/S0263574721000631

[22] Aoustin, Y., Formalskii, A.: Walking of biped with passive exoskeleton: evaluation of energy consumption. Multibody System Dynamics **43**(1), 71–96 (2016) https://doi.org/10.1007/s11044-017-9602-7

[23] Chen, Z., Elyaaqoubi, N.L., Abba, G.: Optimized 3d stable walking of a bipedal robot with line-shaped massless feet and sagittal underactuation. Robotics and Autonomous Systems **83**(1), 203–213 (2016)

[24] Geursen, J.B., Altena, D., Massen, C.H.: A model of the standing man for the description of his dynamic behaviour. Agressologie **17**(12), 63–69 (1976)

[25] Perry, J., Burnfield, J.M.: Gait Analysis Normal and Pathological Function (2nd Ed.), p. 570. Taylor & Francis Group, ??? (2010). https://doi.org/10.1201/9781003525592

[26] Roussel, L., Canudas.De.Wit, C., Goswami, A.: Generation of energy optimal complete gait cycles for biped robots. In: Proceedings. 1998 IEEE International Conference on Robotics and Automation (Cat. No.98CH36146), vol. 3, pp. 2036–20413 (1998). https://doi.org/10.1109/ROBOT.1998.680615

[27] Roussel, L., Canudas.De.Wit, C., Goswami, A.: Comparative study of method for energy-optimal gait generation for biped robots. In: Proceedings. 1997 International Conference on Informatics and Control, St Petersburg, pp. 1205–1212

(1997)

[28] Van.Der.Zee, T., Mundinger, E.M., Kuo, A.D.: A biomechanics dataset of healthy human walking at various speeds, step lengths and step widths. figshare. Collection. **9**(6), 704 (2022) https://doi.org/10.6084/m9.figshare.c.5897423.v1

[29] Van.Der.Zee, T., Mundinger, E.M., Kuo, A.D.: A biomechanics dataset of healthy human walking at various speeds, step lengths and step widths. Science Data **9**(6), 704 (2022) https://doi.org/10.1038/s41597-022-01817-1

[30] Tlalolini, D., Chevallereau, C., Aoustin, Y.: Human-like walking: Optimal motion of a bipedal robot with toe-rotation motion. IEEE/ASME Transactions on Mechatronics **16**(2), 310–320 (2011) https://doi.org/10.1109/TMECH.2010.2042458

[31] De.Cock, A., Vanrenterghem, J., Willems, T., Witvrouw, E., De.Clercq, D.: The trajectory of the centre of pressure during barefoot running as a potential measure for foot function. Gait & Posture **27**, 669–675 (2008)

[32] Aoustin, Y.: Walking gait of a biped with a wearable walking assist device. Int. J. of Humanoid Robotics **12**(2), 1550018–11155001820 (2015) https://doi.org/10.1142/S0219843615500188